JGR Atmospheres

RESEARCH ARTICLE
10.1029/2019JD031203

Special Section:
Long-term Changes and Trends in the Middle and Upper Atmosphere

Twenty-First-Century Changes in the Eastern Mediterranean Etesians and Associated Midlatitude Atmospheric Circulation

Stella Dafka[1], Andrea Toreti[2], Prodromos Zanis[3], Elena Xoplaki[1,4], and Juerg Luterbacher[1,4]

[1]Climatology, Climate Dynamics and Climate Change, Department of Geography, Justus-Liebig-University of Giessen, Germany, [2]Joint Research Centre, European Commission, Ispra, Italy, [3]Department of Meteorology and Climatology, School of Geology, Aristotle University of Thessaloniki, Thessaloniki, Greece, [4]Centre of International Development and Environmental Research, Justus Liebig University of Giessen, Germany

Abstract The Etesians are the dominant synoptically driven winds observed in the Eastern Mediterranean, usually from late spring to late summer. Due to the complex topography, the Etesians can be very strong and pose significant environmental hazards, especially over wildfire incidents. This study assesses the impacts of climate change on future Etesians by analyzing the response of the most recent EURO-CORDEX regional climate simulations at the 12-km grid resolution over the twenty-first century. The mean model ensemble projects a significant increase of the Etesians' frequency and intensity under the two emission scenarios RCP4.5 and RCP8.5. This response is connected to an increase in the zonal wind at 200 hPa, a reinforcement of the midlatitude westerly flow, and a decrease in the wave amplitude. These circulation changes accelerate the mid-to-high latitude eastward propagation of the large-scale circulation systems which can favor enhanced ridges over the Balkans. A strengthening and poleward shift of the subtropical jet stream is also projected, connected with stronger subsidence over the Eastern Mediterranean. The projected changes will have profound environmental and societal implications, including the lengthening of the wildfire season and increasing air pollution risk in the region. On the other hand, the current estimate of future wind power potential in the Aegean Sea will be significantly increased by the end of the century, which might have positive impact in the regional economy.

Plain Language Summary The Etesians are one of the most prominent wind systems in the world. They are persistent, northerly, regional-scale winds that blow every summer over the Aegean Sea and the Eastern Mediterranean. They are known since antiquity, with the first reference dating back to the eighth century B.C. Recent studies based on climate model projections have pointed to a decrease in the wind speed in most of Europe for the coming decades, except for the Aegean Sea. Thus, this study assesses the impacts of climate change on Etesians and identifies the associated dynamical mechanisms. The main findings show an increase in the Etesians' frequency and intensity over the twenty-first century mainly attributable to changes in the large-scale atmospheric circulation. The projected changes will have profound societal and environmental implications in response to the associated lengthening of the wildfire season and the increased risk of air pollution in the region. At the same time, a positive impact on the regional economy due to the increase in wind power potential is also expected.

Key Points:
- The impacts of large-scale atmospheric circulation changes in the Eastern Mediterranean winds over the twenty-first century is here assessed
- Projections show a reinforced westerly flow, a decreased meridional wave amplitude, and an intensified-poleward shifted Subtropical Jetstream
- A progressively increase of Etesians frequency and intensity induced by large-scale circulation processes is projected for the twenty-first century

Supporting Information:
- Supporting Information S1

Correspondence to:
S. Dafka,
styliani.dafka@geogr.uni-giessen.de

Citation:
Dafka, S., Toreti, A., Zanis, P., Xoplaki, E., & Luterbacher, J. (2019). Twenty-first-century changes in the Eastern Mediterranean Etesians and associated midlatitude atmospheric circulation. *Journal of Geophysical Research: Atmospheres, 124,* 12,741–12,754. https://doi.org/10.1029/2019JD031203

Received 19 JUN 2019
Accepted 1 OCT 2019
Accepted article online 22 OCT 2019
Published online 9 DEC 2019

1. Introduction

The Etesians are an integral summer feature of the regional climate of the Eastern Mediterranean (EMED) that is influenced by interactions between midlatitude and tropical processes (Cherchi et al., 2014; Logothetis et al., 2019; Tyrlis et al., 2013). Tyrlis and Lelieveld (2013) suggested that both the Etesians and the upper level subsidence over the EMED are manifestations of the Rossby wave structure induced by the monsoon convection. The recurrent EMED summer circulation and, thus, the Etesians are associated to the stability of the monsoon signal.

The conditions necessary for the establishment of the Etesians are a stationary high-pressure system centered over central Europe and the Balkans and a thermal low (Anatolian low) that extends westward from the Arabian Peninsula over the EMED. This dipole induces a synoptic pressure gradient over the Aegean

Sea that drives surface winds into the Archipelago from the northeast quadrant. Air flowing over the complex topography is channeled and accelerated through passes and rocky mountains, notably in the Aegean islands (Kotroni et al., 2001). The Etesians regime displays distinct seasonal variation, blowing persistently from May through September, and usually peaks during July and August (Dafka et al., 2016). Episodes are typically associated with strong, gusty winds and very low relative humidity (Tyrlis & Lelieveld, 2013).

Among the most notorious environmental hazards associated with Etesians are wildfires. The Etesians induce the greatest fire risk when they coincide with low humidity during the peak period (Amraoui et al., 2013). The intense winds can rapidly spread the fire rendering the wildfire predictions and firefighting extremely difficult, which could result in significant loss of life and property (Koletsis et al., 2009; Kotroni et al., 2001). Another environmental impact concerns the contribution to the transport of pollutants such as ozone and other anthropogenic aerosols, from central Europe and the Balkans over the EMED (Georgoulias et al., 2016; Zanis et al., 2014).

Due to the complex topography and the scarcity of the data, only few studies have investigated the projected changes in regional wind systems over the Mediterranean basin. For instance, Regional Climate Model (RCM) simulations project a significant decrease in Tramontane frequency over the gulf of Lion (Obermann-Hellhund et al., 2017) and in the number of Bora events over the Adriatic region (Belušić Vozila et al., 2019) during the twenty-first century. As for the eastern Mediterranean, to date as far as we know, only Anagnostopoulou et al. (2014) and Tolika et al. (2015) based on the RCM RegCM3 and Ezber (2018) using a set of EURO-CORDEX and CMIP5 models assessed future changes of Etesians. They have found an intensification of the Etesians, which was mainly attributed to the strengthening of the high pressure system over the Balkans and the deepening of the Anatolian low. Nevertheless, both studies did not investigate the forcing mechanisms underlying the changes. Our approach goes beyond these findings and provides new evidence of possible changes in Etesians at monthly scale, considering an ensemble of EURO-CORDEX twenty-first century simulations under the two Representative Concentration Pathways (RCP) 4.5 and 8.5.

Changes in the Etesians depend on several competing factors, including changes in the midlatitude circulation (atmospheric blocking activity, midlatitude westerlies), in the jet streams patterns as well as in the Indian summer monsoon variability. Therefore, the major challenge in investigating the Etesians under a changing climate stems from the need: to improve our understanding of the dynamical processes behind the phenomenon and their representation in the RCMs. Indeed, the RCMs should be able to resolve not only the large-scale atmospheric features, such as the development and movement of the large-scale dipole that controls the Etesians, but also the local circulation features that are affected strongly by the complex topography of the Aegean Sea (Dafka et al., 2017). This contribution goes beyond the state of the art through studying changes in the large-scale processes associated with Etesian events and identifying the mechanism behind these changes.

The paper is organized as follows: sections 2 and 3 deal with the description of the data and the analysis performed. Section 4 provides the main results in terms of (1) differences between twenty-first and twentieth-century climatologies, (2) analysis of meridional circulation changes in the area, and (3) changes in the locations and strength of the jet stream patterns. Finally, sections 5 and 6 present the discussions and the conclusions.

2. Data

Our analysis uses historical simulations and future projections driven by nine General Circulation Models (GCMs) available from the fifth phase of the Climate Model Intercomparison Project (CMIP5, Taylor et al., 2012). The selected GCMs provide boundary conditions to four RCMs from the EURO-CORDEX initiative (Jacob et al., 2014) with a spatial resolution of 0.11° (around 12 km). Table 1 provides an overview of all GCM-RCM combinations used in this study. A subset of six models (gray box; Table 1), driven by those EURO-CORDEX RCMs (i.e., the RCA4 and HIRHAM5) that have been already proven to capture the Etesian wind pattern and the associated large-scale circulation within the observational period 1989 to 2004 (Dafka et al., 2017), is selected and used for the analysis.

Table 1
List of GCM-RCM Combinations, Along With the Institution Name and the Corresponding References

Driving GCM	RCM	Institution	Reference
CNRM-CM5	RCA4	Swedish Meteorological and Hydrological Institute (SMHI)	Samuelsson et al. (2011)
EC-Earth	RCA4		
HadGEM2-ES	RCA4		
IPSL-CM5A-MR	RCA4		
MPI-ESM-LR	RCA4		
EC-Earth	HIRHAM5	Danish Meteorological Institute (DMI)	Christensen et al. (2006)
IPSL-CM5A-MR	WRF3.3.1	Institut Pierre Simon Laplace/Institut National de l'Environnement Industrie et des Risques (IPSL/INERIS)	Skamarock et al. (2008) and Menut et al. (2013)
CNRM-CM5	ARPEGE5.2		
CNRM-CM5	ALADIN5.3		

Note. The subset of six models that has been used for the mean ensemble analysis is identified by the gray box.

We study future conditions of mean Sea Level Pressure (SLP), surface zonal (u) and meridional (v) wind components (10 m above surface), geopotential height at 500 hPa (Z500), and zonal and meridional wind components at 200 hPa (U200 and V200, respectively). Changes are calculated for 2021–2050 (mid-21c) and 2071–2100 (late-21c) relative to 1971–2000 (late-20c), under the midrange mitigation (RCP4.5) and high-end (RCP8.5) emission scenarios (Moss et al., 2010). All variables are taken from May to September, at 12 UTC (15:00 local time) when the wind is supposed to reach the highest intensity, due to the daytime deepening of the Anatolian thermal low (Tyrlis & Lelieveld, 2013). In addition, 3-hourly SLP data for the stations of Elliniko and Rhodes are taken from the National Hellenic Meteorological Service.

3. Methods

3.1. Classification of Etesians

The literature describes a wide range of approaches to objectively classify the Etesians (Tyrlis & Lelieveld, 2013). Here in order to be consistent with our previous studies (Dafka et al., 2016, 2017, 2018), we define intense Etesians as days exceeding the third-quartile (Q3) threshold of 12 UTC observed/simulated SLP differences (ΔP) between Elliniko (PE) and Rhodes (PR; $\Delta P = PE - PR \geq Q3$). Likewise, days such that *median* $\leq \Delta P < Q3$ are defined as moderate Etesians. Days with negative ΔP indicate southerlies and are excluded from the analysis. Finally, following *Tyrlis and Lelieveld* (2013), an Etesian episode is defined as a sequence of intense Etesian days ≥2. Table 2 presents Etesians' classification as derived from the observed Etesian days. Note that the selection of the Etesians was done using the corresponding value of Q3 and median of each period (late-20c, mid-21c, and late-21c). A detailed description of the classification method can be found in Dafka et al. (2016, 2017, 2018).

3.2. Mean Model Ensemble

The Mean-Model Ensemble (MME) of six GCM-RCM combinations (gray box; Table 1) is analyzed regarding changes of Etesians frequency, wind speed, SLP, Z500 anomalies, and U200 under the two RCPs 4.5 and 8.5 for the mid- and late-21c. The magnitude of the change is calculated as the difference between the reference 30-year period (1971–2000) and the two future 30-year periods (2021–2050 and 2071–2100). Model ensemble allows to sample part of models' structural uncertainty (Knutti et al., 2010, 2017), to evaluate the model spread and investigate the robustness of signals. In this study, the projected changes are robust and consistent if at least 66% of all simulations agree in the direction of change and at least 66% of the simulations show significant changes at the 90% level using the *Wilcoxon–Mann–Whitney* test (Pfeifer et al., 2015). Our analysis considers also the results of individual models (apart from the MME). We extend prior findings (Anagnostopoulou et al., 2014; Ezber, 2018) by considering changes in the waviness of the atmospheric circulation as well as in the strength and locations of the jet streams and their implications on Etesians, as described in the following sections.

3.3. Z500 Wave Extent

In order to assess whether the wave amplitude (i.e., the meridional extent) of the 500 hPa field of the Etesian days is projected to change, we use the metric proposed by Barnes (2013). More specifically, a single isopleth

Table 2
Classification of Observed Etesian Days for the Extended Summer Season May to September in the Period 1971–2000

Condition	Name of class	Percentage of observed Etesian days and number of episodes in late-20c
$\Delta P < 0$	Southerly flow	10.3%
Median $\leq \Delta P < Q_3$	Moderate Etesians	22.0%
$\Delta P \geq Q_3$	Intense Etesians	22.5%
Intense Etesian days ≥ 2	Etesian episodes	253

for each summer month is used and its maximum and minimum latitudes ($\overline{Lat}(max)$ and $\overline{Lat}(min)$, respectively) are calculated over the EURO-CORDEX domain. The meridional wave extent is then defined as the difference (ΔLat) of the averaged maximum and minimum latitudes, $\overline{Lat}(max)$ and $\overline{Lat}(min)$, during the intense Etesian days:

$$\Delta Lat = \overline{Lat}(max) - \overline{Lat}(min)$$

Following the methods of Francis and Vavrus (2012, 2015) and Barnes (2013) single isopleths at 500 hPa were selected. The MME climatology of the geopotential height at 500 hPa and zonal wind at 200 hPa from the model simulations are calculated. Then, those Z500 isopleths that exist in the strongest mean U200 summer climatology and, thus, could be used as a proxy for the trajectory of the upper level jet stream are selected. Results are presented as the average meridional extent of these isopleths (in our case are the 5650, 5700, 5750 m for each month). This analysis is performed from July to September.

3.4. Meridional Circulation Index

A key question that remains unexplored in the linkage between Etesians and the midlatitude atmospheric circulation is whether a stronger midlatitude westerly flow can both accelerate the eastward propagation of synoptic systems and amplify the high-pressure system over the Balkans. In addition, a stronger subtropical jet stream could be associated with an amplified trough over the EMED that enhances the Etesians. To address these questions, we calculated the Meridional Circulation Index (MCI) following Francis and Vavrus (2015). The MCI is a simple metric that estimates departures from the zonal flow of the upper level winds and it is defined as

$$MCI = \frac{V|V|}{U^2 + V^2}$$

where U and V are the zonal and meridional components of the wind at 200 hPa, respectively. When MCI = 0, the wind is zonal, and when MCI = 1 (−1), the wind is blowing from the south (north). Positive (negative) differences of |MCI| in the projected future time periods relative to the historical simulations indicate more (less) undulations, suggesting an increased meridional (zonal) circulation.

3.5. Jet Strength and Position

Our analysis derives daily time series of the strength and the latitudinal/longitudinal position of the Polar and Subtropical Jet streams (PJ and STJ, respectively). We examine the projected changes under both RCPs and future periods and we quantify the trends in their position (meridional and zonal location) and strength.

Both jets are best diagnosed from the wind at higher levels. Therefore, the latitude/longitude and wind speed of the jet streams are identified in daily U200 over the extended summer period (May to September). In order to select the preferred position of the jet streams during the Etesians, the MME climatology of the zonal wind at 200 hPa from the historical simulations is calculated. Results have shown that, during the Etesians and in all months, the PJ is confined to the area 0°–20°E and latitude from 50°–60°N. The STJ has a preferred position, ranging 18°–38°E and 32°–42°N (in agreement with Dafka et al., 2016). Generally, both jets tend to be weaker in summer as compared to winter. Using the method of Woollings et al. (2010), our analysis consists of the following steps:

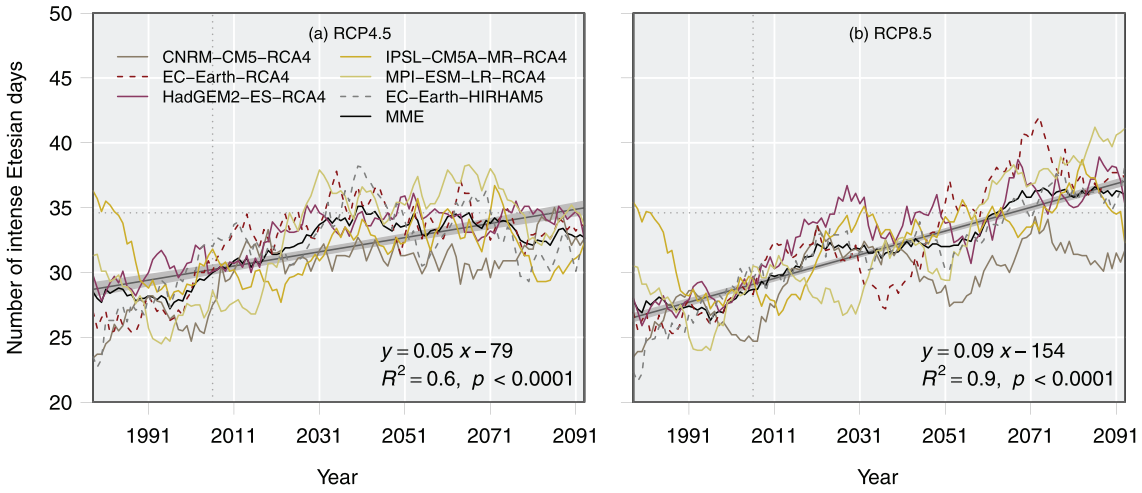

Figure 1. The 15-year running mean of intense Etesian days per year in historical runs and (a) RCP4.5 and (b) RCP8.5 runs. Horizontal dotted line shows the mean of observed Etesian days during the period 1971–2000. The vertical dotted line marks the starting point of climate projections. Gray lines show the MME linear trend.

1. The daily mean zonal wind at 200 hPa is zonally and meridionally averaged for the identification of the latitude and longitude, respectively, over the longitudinal sector 0°–20°E (18°–38°E) as a proxy for the location of the PJ (STJ), neglecting winds poleward of 60° (42°) and equatorward of 50° (32°N);
2. The intense Etesian days are selected;
3. The jet speed is then identified as the maximum westerly wind speed of the selected days. The jet latitude and longitude are defined as the latitude/longitude at which the maximum jet speed is found.

4. Results

4.1. Intense Etesian Days

Figure 1 shows the 15-year running mean of intense Etesian days per year for each GCM-RCM and the MME in historical runs, RCP4.5 (Figure 1a) and RCP8.5 (Figure 1b).

The MME projects a statistically significant (p value $\leq$0.05) annual increase of about 0.3% (0.15%) in the number of Etesian days for the twenty-first century compared to late-20c under RCP8.5 (RCP4.5). The increase under RCP4.5 can be seen only until mid-21c, while the Etesian days remain constant thereafter (Figure 1a). It is worth to note that RCP4.5 emissions peak around 2040 and diminish afterward. At monthly scale (where the full period is May–September), the MME shows a robust and statistically significant increase in the Etesian days in September of about 2 and 4% for mid- and late-21c, in both RCPs. A robust and statistically significant increase (of about 3%) in the Etesian days is found also for May and June, but only in late-21c under RCP8.5. In contrast, a robust and statistically significant reduction of about 5% is identified in August in late-21c under RCP8.5. While the frequency of the Etesian episodes is increased (except for August), there is no consistent evidence for changes in the episodes' duration (i.e., the number of consecutive days) in any of the RCPs or future periods.

Generally, these results show that the contribution of intense events to the summer seasonal amounts will significantly increase over the century. This phenomenon is more pronounced in May, June, and September in late-21c under RCP8.5, suggesting a strengthening of Etesians activity outside of the traditional peak period (July–August). The projected changes under the RCP8.5 are approximately double than the ones from the midrange mitigation emission scenario RCP4.5 (Figure 1).

4.2. Mean Model Ensemble

We investigate projected changes of the surface wind and the large-scale circulation patterns associated with Etesians. Figure 2 shows the MME future changes in wind speed (Figures 2a–2d), SLP (Figures 2e–2h), Z500 anomalies (Figures 2i–2l), and U200 (Figures 2m–2p) for the intense Etesian days for each month (the peak months, July and August, present similar characteristics and, thus, are considered together), for late-21c

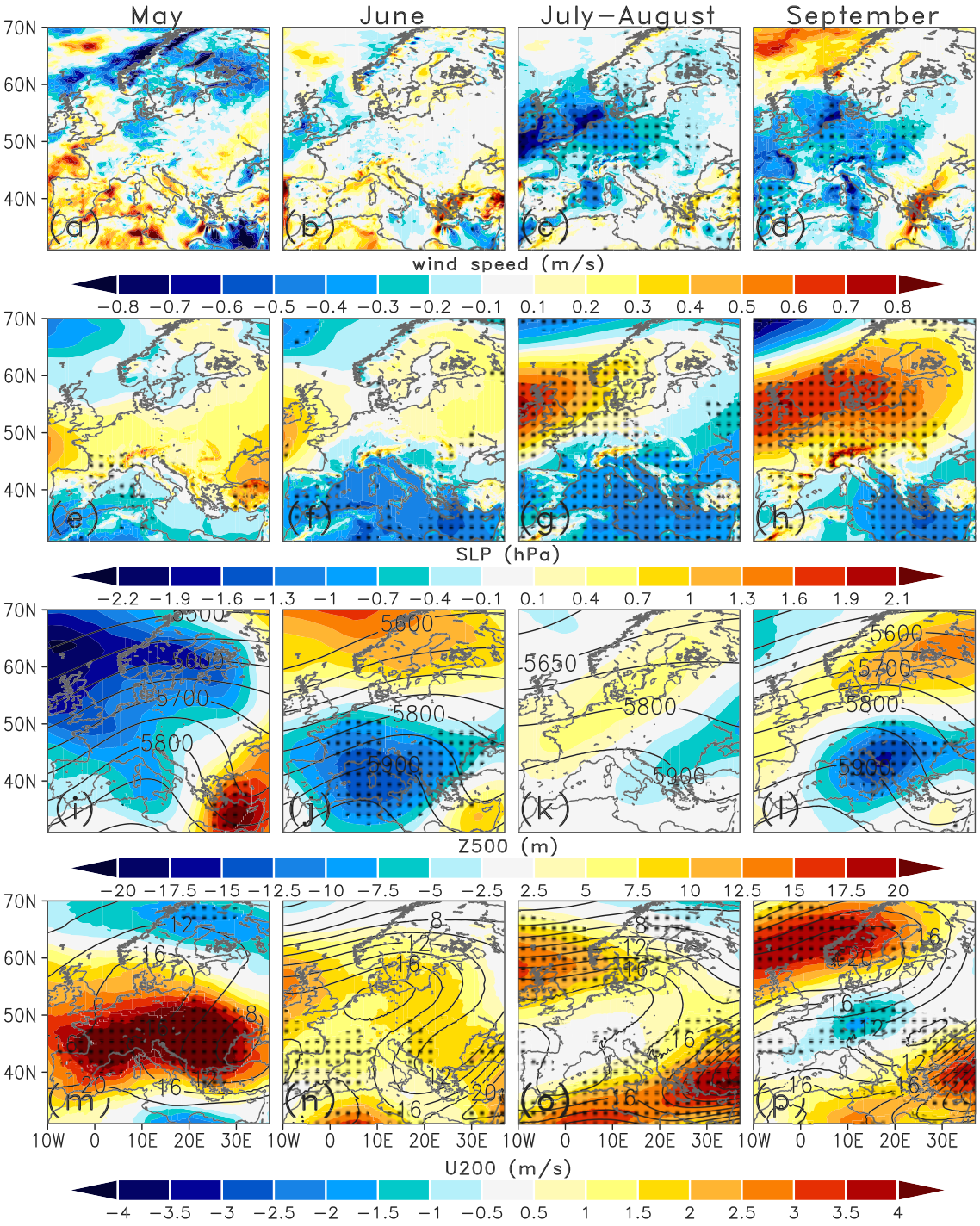

Figure 2. MME future changes in (a–d) wind speed (m/s), (e–h) SLP (hPa), (i–l) Z500 anomalies (gpm), and (m–p) U200 (m/s), for the late-21c (2071–2100) relative to the late-20c (1971–2000) under RCP8.5 for the intense Etesian days per month. Contours indicate the MME climatological values in RCP8.5 for (i–l) Z500 and (m–p) U200. Stippling indicates robust (66% of the models) and statistically significant changes at 90%.

relative to late-20c under RCP8.5. Projections indicate a strengthening of the Etesian wind speed over the Aegean Sea of about 0.5–1 m/s, which is robust and statistically significant in the period June to September (Figures 2b–2d; see also Figure S1 for a spatial focus over the Aegean Sea). On the contrary, in July to September (Figures 2c and 2d) near-surface wind speeds over most of the European areas are projected to decrease.

Sea level pressure patterns associated with Etesians for late-21c compared to late-20c under RCP8.5 indicate robust and statistically significant increase of SLP over the British isles, the North Sea, and central Europe in July–August (Figure 2g) and over western and northern Europe in September (Figure 2h). The SLP is projected to decrease in the EMED in the period June to September (robust and statistically significant results; Figures 2f–2h). Indeed, over most of central and western Europe, the subtropical high pressure system is projected to strengthen by the end of the century by ~1.5–2 hPa, while the MME projects a deepening of the EMED low-pressure system by ~1–1.5 hPa, indicating a strengthening of the westward extension of the Anatolian thermal low. Overall, from July to September the dipole that sustains the Etesians is enhanced, leading to an intensification of the pressure gradient over the Aegean, and therefore to stronger surface northerlies.

All GCM-RCM combinations represent the typical 500-hPa atmospheric dipole that is associated with Etesians very well in the late-twentieth century (not shown). The configuration is characterized by strong and broad positive 500-hPa geopotential height anomalies over central Europe and a deepening of the 500-hPa trough over the EMED (not shown). Late-21c projections relative to late-20c show that the anomalous ridge weakens and extends southwestward and northeastward, connected to stronger midlatitudes westerlies at 500-hPa level (Figures 2j–2l). The central European ridge is shifted northward, associated with negative anomalies over central and southern Europe. Z500 patterns are consistent with the regional SLP signal, which shows an intensification over central and western Europe in July–August and September (Figures 2g, 2h, 2k, and 2l). Except for May (Figure 2i), no statistically significant changes are found in the 500-hPa anomalous EMED trough.

In agreement with the lower and midtropospheric changes, large-scale circulation in the upper troposphere will also experience significant changes in the future. The MME shows a notable increase in U200 (larger than 3 m/s) around 60°N and along 35°N, which is robust and statistically significant for the period July to September (Figures 2o and 2p). In May and June, results show a strengthening of U200 in late-21c compared to late-20c especially over the central Europe and the Balkans (Figures 2m and 2n). All variables exhibit the same direction of change, of weakened magnitude under the moderate scenario (RCP4.5; not shown).

Six out of nine GCM-RCM combinations (except for IPSL-CM5A-MR-WRF331, IPSL-CM5A-MR-RCA4, and CNRM-CM5-ARPEGE5.2 from Table 1) agree in the direction and magnitude of change regarding the intense Etesians wind speed in late-21c under RCP8.5 (not shown). The projected changes regarding the wind speed and the SLP (U200) are already apparent in the mid-21c for both RCPs, while the signal is robust and statistically significant from June to September (July to September).

To assess the MME projected changes with respect to the pressure gradient over the Aegean Sea, we consider also the moderate Etesian days. The MME projected changes have the same sign in both future periods and RCPs (for RCP8.5; see Figure S2) and demonstrate enhanced magnitude for each variable under moderate Etesians compared to the intense Etesians. The latter strengthens confidence that the projected changes are robust and independent of the pressure gradient.

4.3. Z500 Wave Extent

We extend our analysis by presenting atmospheric waviness as a function of 500-hPa wave extent to identify potential changes in the midlatitude meridional circulation across the EURO-CORDEX domain. Table 3 shows the projected changes in ΔLat in late-21c relative to late-20c for each ensemble member and the MME in July, August, and September.

All GCM-RCM combinations (except for the EC-Earth-HIRHAM5) show a decrease in the meridional wave amplitude in both RCPs. The MME suggests a decrease in late-21c (mid-21c; not shown) of about 1.3–1.7 under the RCP8.5 and 0.7–1.1 under the RCP4.5, compared to late-20c, which potentially indicates a tendency of less undulations (waviness) in the future. This phenomenon can promote the eastward progression of the disturbances reaching central Europe and the Balkans, which is also coherent with the intensification of the SLP dipole seen at the surface (Figures 2g and 2h).

Figure 3 shows the time series of the meridional wave extent (ΔLat) of Z500. The MME shows a downward trend of ΔLat in both future periods and RCPs; however, statistically significant results are obtained only in mid-21c under RCP4.5 (0.6° decade^{-1}; Figure 3a) and in late-21c under RCP8.5 (0.5° decade^{-1}; Figure 3b).

Table 3
Future Changes in ΔLat (°) in Late-21c Relative to Late-20c for Each Ensemble Member and MME Under RCP4.5 and RCP8.5 for July, August, and September

	RCP4.5			RCP8.5		
ΔLat (°)	July	August	September	July	August	September
CNRM-CM5-RCA4	−4.5	−1.2	−3.1	−1.3	−1.4	−1.7
EC-Earth-RCA4	−0.5	−0.6	1.4	−2.7	−1.7	−2.5
HadGEM2-ES-RCA4	−0.6	−1.7	−1.7	−2.2	−2.5	−5.1
IPSL-CM5A-MR-RCA4	−0.1	−0.1	−1.5	−1.0	−0.3	−3.1
MPI-ESM-LR-RCA4	−1.3	−2.1	−1.6	−1.6	−3.3	−2.9
EC-Earth-HIRHAM5	0.6	1.1	2.5	−0.3	1.5	5.5
MME	−1.1	−0.8	−0.7	−1.5	−1.3	−1.7

4.4. Meridional Circulation Index

Here we analyze the MCI index in order to obtain more information on the spatial variation of waviness over the European sector during the intense Etesian days (Figure 4).

The MME projected changes of |MCI| at 200 hPa for the late-21c in both RCPs show predominantly decrease over the EMED (robust and statistically significant in the period June to September; Figures 4b–4d and 4f–4h). These areas are closely matched by the spatial pattern of U200, as seen in Figures 2n–2p, indicating increased zonal circulation and suggesting, thus, an intensified STJ which might be one factor driving more subsidence and northerly flow over the Aegean Sea. The identified areas are also broadly consistent with the surface pressure signals presented in Figures 2f–2h. The EMED sector exhibits a reinforced low-pressure system. In addition, in July–August the Euro-Atlantic sector exhibits negative |MCI| values which correspond to a reinforced westerly flow in late-21c under RCP8.5 (Figure 4g).

Overall, the zonal flow at 200 hPa shows *enhanced* westerly jet over the EMED near 35°–40°N in June to September, stretching across most of the Mediterranean Sea in July and August. The response at approximately 50°N shows similarities in the peak period with either a slightly reinforced westerly flow, potentially associated with decreased waviness. Finally, similar |MCI| changes are projected during the mid-21c, although the signal is not statistically significant.

4.5. Jet Strength and Position

In order to better understand the changes identified in the large-scale circulation, the Z500 wave amplitude, and the MCI, the link between the intense Etesians and the jet streams' strength and position is analyzed.

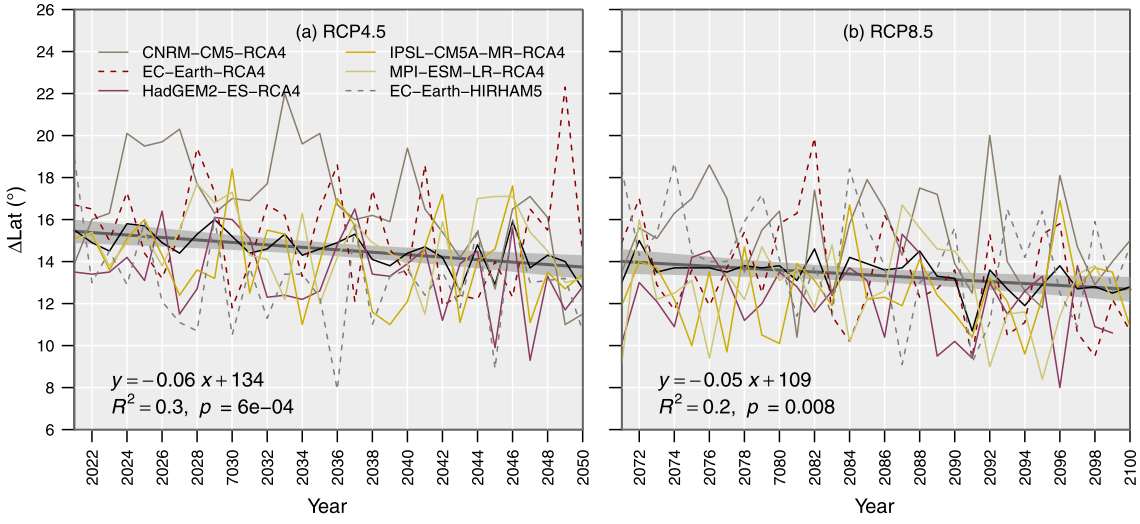

Figure 3. Interannual variability of ΔLat (°) in (a) mid-21c under RCP4.5 and in (b) late-21c under RCP8.5 for each ensemble member. Gray lines show the MME linear trend.

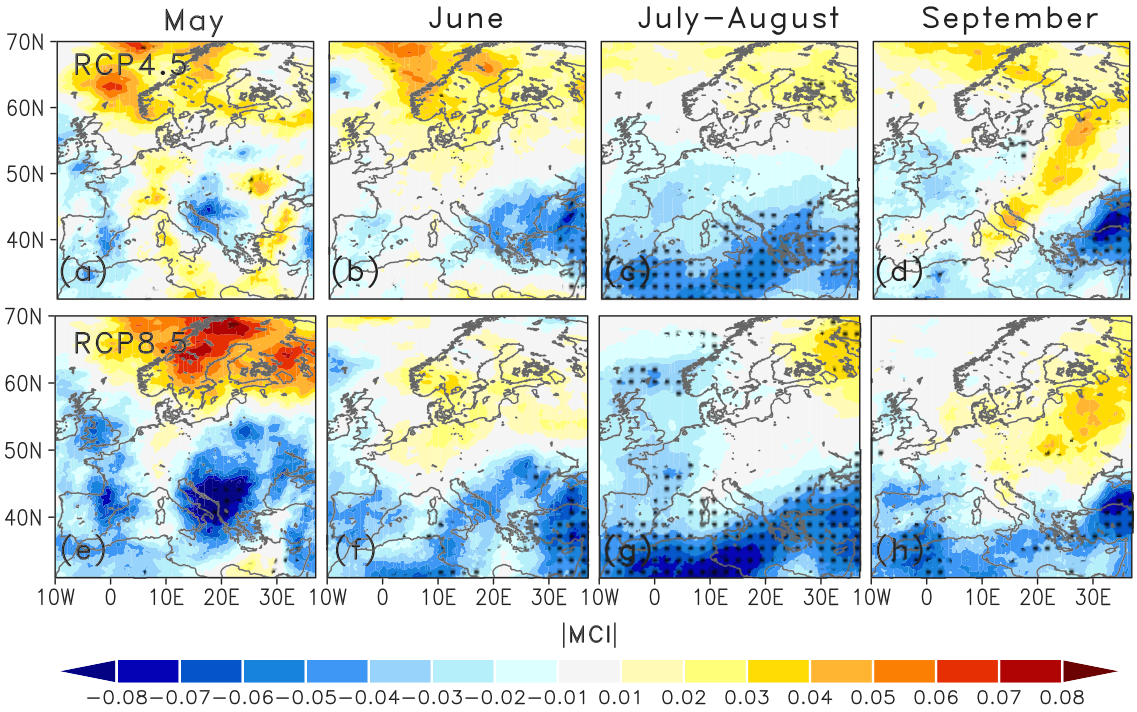

Figure 4. MME projected changes of |MCI| at 200 hPa for late-21c relative to late-20c under (a–d) RCP4.5 and (e–h) RCP8.5 for the intense Etesian days per month. Stippling indicates robust and significant changes at 90%.

The jet stream response under RCP4.5 and RCP8.5 is examined in each GCM-RCM combination by looking at speed, latitude, and longitude and the MME annual trends. In the RCP8.5, all models project an average increase in the STJ strength in late-21c (mid-21c) of about 1.4 m/s (0.3 m/s) compared to late-20c in July to September. The MME shows a positive trend in the STJ strength under RCP8.5, which is found robust and statistically significant only in the mid-21c (0.6 m/s per decade; Figure 5a). Results under RCP4.5 suggest a strengthening in the STJ wind speed of up to 0.9 m/s in late-21c and in July to September (not shown). August and September are the months with the highest strengthening under both RCPs and future periods.

As for the PJ strength, the MME projects an average increase in the jet wind speed by the end of the century (mid-21c) of 3.5 m/s (1.4 m/s) compared to late-20c. The IPSL-CM5A-MR-RCA4 shows the highest increase in the PJ wind speed. In addition, the MME suggests a robust and statistically significant positive trend in the PJ strength of 0.8 m/s per decade for late-21c under RCP8.5 (Figure 5b). The MME under RCP4.5 shows also an increase in the PJ wind speed of approximately 1.5 m/s in both future periods; however, no significant trends are found under this scenario (not shown). The greatest increase in the PJ wind speed is found in June (June and September) under RCP8.5 (RCP4.5) for both future periods.

The STJ during the extended summer period of late-20c displays an average meridional (zonal) location at 37°N (31°E) and shifts northward (eastward) during mid and late-21c at 38°N (32.5°E). The mean position of the PJ (54.5°N and 9.3°E) shows no or little variation in the future compared to the recent past. Figure 6 shows the projected changes in meridional location of STJ in mid-21c and late-21c relative to late-20c under RCP4.5 and RCP8.5 for the MME and each ensemble member per month.

Most of the models suggest a poleward shift (~0.3°) of the STJ under both RCPs and future periods compared to late-20c. This can be seen, with some exceptions (especially in EC-Earth-RCA4 and IPSL-CM5A-MR RCA4) in all months (Figures 6a–6d); however, it is more pronounced in May and September. Regarding the longitude, the MME shows an eastward shift of the STJ at a rate of ~0.8° (more pronounced in September; not shown). The MME shows a statistically significant negative trend of of about 0.4° STJ-Lon in late-21c under RCP8.5.

The projected changes in the PJ latitude and longitude show large variation among the models and months (not shown). Most models show an eastward (westward) displacement in August (May and September)

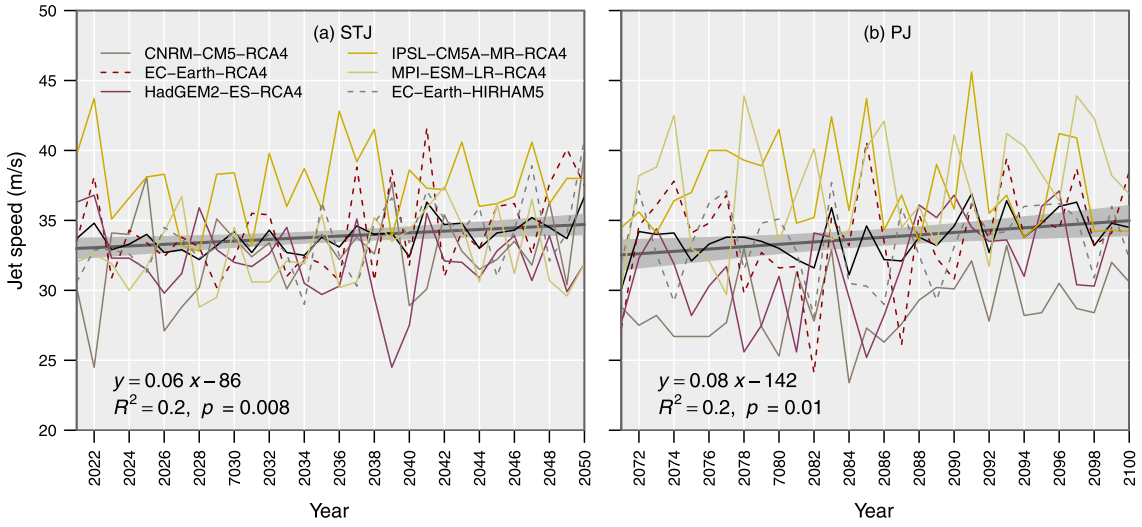

Figure 5. Interannual variability of mean wind speed (m/s) of (a) STJ in mid-21c and (b) PJ in late-21c under RCP8.5 for each ensemble member. Gray lines show the linear trend.

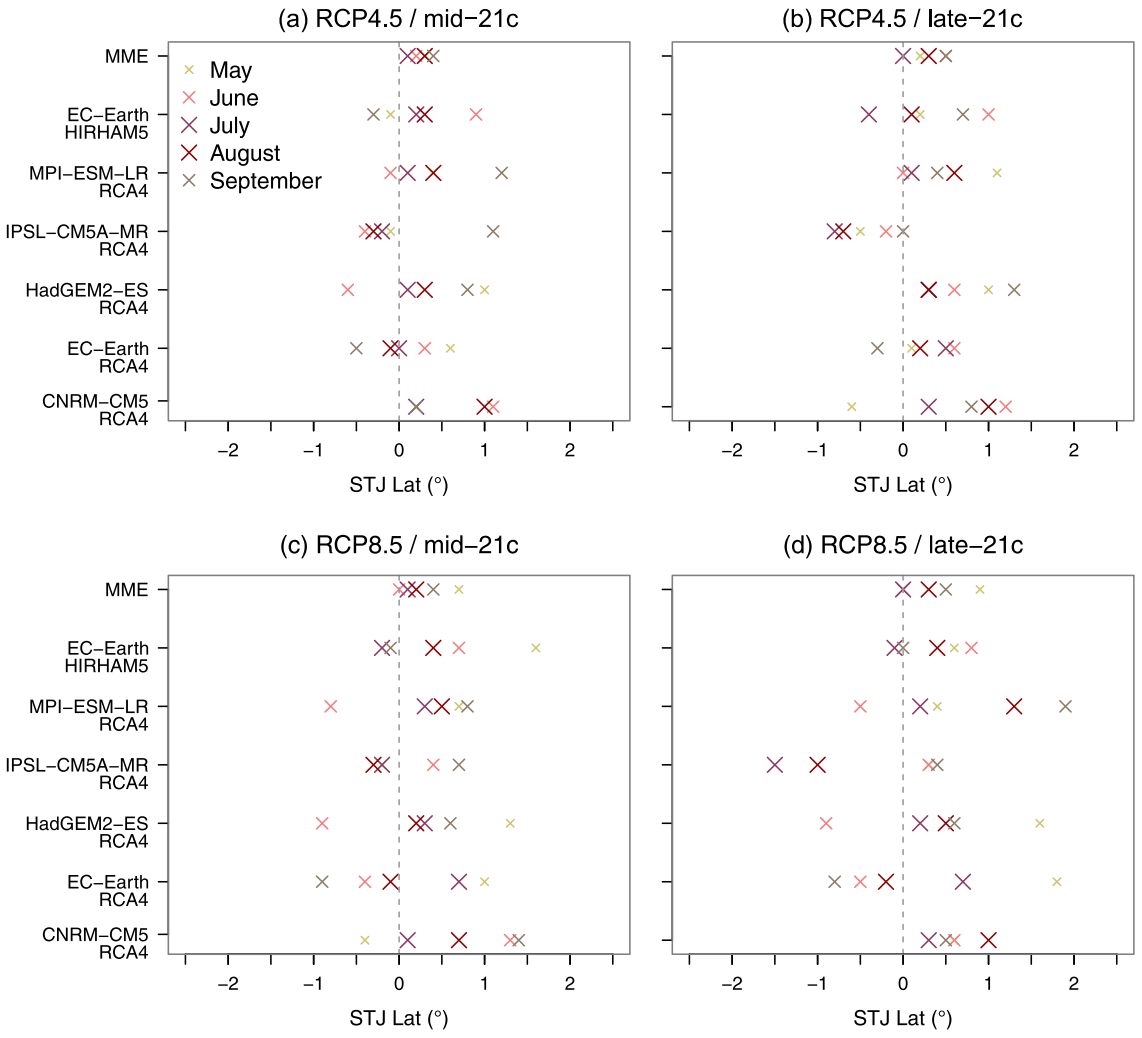

Figure 6. Projected changes in meridional location of STJ Lat (°) for the MME and each ensemble member in (a and c) mid-21c and (b and d) late-21c relative to the late-20c under (top panel) RCP4.5 and (bottom panel) RCP8.5 for each ensemble member and month.

under RCP8.5 (both RCPs) and both future periods. There is an agreement on the southward (poleward) PJ shift in May (June–September) in late-21c under RCP8.5. In addition, the MME shows a statistically significant upward trend of PJ-Lon in late-21c under both RCPs. A negative trend in the PJ-Lat in late-21c under both RCPs is also indicative, though not significant.

Overall, the MME shows statistically significant intensification and an eastward shift of the PJ under both RCPs and future periods. In addition, the STJ is projected to increase especially in July to September and moves northward in both RCPs and future periods. The dominant signal implies acceleration in eastward wave propagation and increased subsidence over the EMED.

5. Discussion

Driven by strong emission-related forcing, the simulated surface wind and the large-scale atmospheric circulation associated with Etesians features major changes by the end of the century.

Our analysis shows that most GCMs-RCMs agree on the progressive increase of Etesians days. This increase, which is clearly evident in the twenty-first century under RCP8.5, is particularly noticeable in September and less pronounced in May–June. In contrast, a considerable decrease in Etesians frequency is found in August. The MME projects an increase in the Etesians wind speed in the period June to September in both future periods under RCP8.5. Extreme wind events are expected to become more (less) frequent and more intense in May, June, and September (July–August) by the end of the century. Changes are associated with an amplification of the large-scale SLP dipole that controls the pressure gradient over the Aegean Sea and, thus, the Etesians. We expect a large-scale decrease of SLP over the EMED, associated with a deepening of the Anatolian thermal low (in agreement with Anagnostopoulou et al., 2014 and Ezber, 2018). Sandeep and Ajayamohan (2015) investigated the SLP linear trend during the period 2006–2099 under RCP8.5 using a MME of 23 CMIP5 simulations and identified also a significant decrease over the EMED. In addition, Hochman et al. (2017) analyzed an ensemble of eight CMIP5 models and found that in summer the occurrence of the Persian Trough (Anatolian low) over the EMED is expected to be lengthened by 49% at the end of the century under RCP8.5.

Changes seen at the surface wind field are inherited from the large-scale circulation processes. We find that the midlatitude sinuosity (seen as reduced north-south deviations of the geopotential height isopleths at 500 hPa) associated with Etesians is projected to decrease in response to climate change according to the EURO-CORDEX simulations. The EC-Earth-HIRHAM deviates from the MME; however, its driving GCM exhibits biases in the representation of the mean state of the geopotential height at 500 hPa over the Euro-Atlantic region (Hartung et al., 2017), and thus, this model should be treated with caution. Di Capua and Coumou (2016) found significant downward trends in meandering over the Eurasian sector during summer, which is consistent with the recently reported decrease in summer synoptic activity (Coumou et al., 2015). In addition, many previous studies based on CMIP5 model runs have found a robust decrease in wave extent (Barnes & Polvani, 2015; Cattiaux et al., 2016) and a decrease in European blocking frequency by the end of the twenty-first century (Barnes & Polvani, 2015; Masato et al., 2013). We extend previous analyses, by assessing the implications of changes of the midlatitude circulation to a specific regional wind system, that is, the Etesians.

Atmospheric circulation changes in the mid-troposphere are already noticeable in late-20c and were mainly attributed to anthropogenic warming (Christidis & Stott, 2015). As for the future, climate models predict a robust poleward shift of the jet streams during the warm season in response to anthropogenic forcing (Barnes & Polvani, 2015; Peings et al., 2017; Woollings & Blackburn, 2012). Nevertheless, there is a lack of consistency among the CMIP5 models regarding the zonal wind responses at 200 hPa (Barnes & Polvani, 2015; Yim et al., 2016). We find the strengthening of both jet streams and the northward displacement of the STJ in both RCPs and future periods, when the Etesians are blowing. It is noteworthy to mention that both jet streams are sufficiently captured in the EURO-CORDEX simulations within the historical period 1989–2004 (Dafka et al., 2017). This increases the confidence in the projected signal. Time series of jet locations from individual models (not shown here) show that at least 66% of models used for the study reproduce STJ's poleward shift in the period July to September. The projected zonal mean changes seem favorable for an intensification of the Etesians. Our findings are consistent with Coumou et al. (2014) who showed that the July–August thermal gradients are generally projected to increase northward of 50°N leading to

strengthening of the polar jet. In addition, Coumou et al. (2018) reported that during summer the subpolar westerlies around 70°N along with the distinct subtropical jet stream form a double-jet regime, which promotes the development of resonant flow regimes. While recently, Mann et al. (2017), using CMIP5 simulations have shown that the double-jet patterns have been turning up more often in the summer months due to high-latitude land warming. Barnes and Polvani (2015) have found a northward displacement of the PJ over the North America/North Atlantic sector in summer. In contrast, our results regarding the PJ shift in latitude and longitude vary across models and months, and the signal is not clear, at least during the Etesians. We cannot confirm that the jets will form a double-jet regime more often in the upcoming decades. Nevertheless, the concurrent variation between the STJ and PJ is proven to act as an important signal associated with increased subsidence and extreme wind events over the Aegean Sea during the boreal summer.

Overall, the Etesian response to climate change is associated to stronger zonal flow, reduced waviness, and northward displacement of the STJ. This mechanism is consistent with the upper tropospheric warming in the tropics that induces both a poleward shift and a strengthening of the westerly flow (Cattiaux et al., 2016; Peings et al., 2017), and with the projected decrease in European blocking frequency seen in the twenty-first century based on CMIP5 model runs (Barnes & Polvani, 2015; Masato et al., 2013; Matsueda & Endo, 2017; Woollings et al., 2018). The reduced blocking activity in summer facilitates the easterly propagation of the synoptic activity and, therefore, favors the formation of the Etesians (Tyrlis et al., 2015).

Atmospheric circulation changes both in the middle to upper troposphere vary insignificantly (to some extent) from one ensemble member to the other, highlighting low uncertainties in projected changes in the midlatitude circulation.

Large-scale circulation changes pose also a significant challenge for wind energy production. Previous studies have shown a robust signal for increase wind power generation potential over the EMED in summer, and in particular over the Aegean Sea associated with the Etesian winds (Bloom et al., 2008; Hueging et al., 2013; Koletsis et al., 2016; Moemken et al., 2018; Tobin et al., 2014, 2016). Indeed, the Aegean Sea enjoys a remarkable wind resource, while the average wind speeds (at wind turbines hub height of 80 m) often exceed the 11 m/s, during the intense Etesians (Dafka et al., 2018). Future anthropogenic emissions will change the strength of near-surface winds, at desirable wind turbine sites. It is, therefore, very important to take into account the potential impacts of climate change in the preconstruction wind energy assessment over the Aegean Sea.

6. Conclusions

In this study, we used an ensemble of six GCM-RCM model chains from EURO-CORDEX to estimate future changes of Etesians for the mid- and late-21c under RCP4.5 and RCP8.5. More specifically, we analyze the ensemble mean response regarding changes in Etesians' frequency, intensity, and the associated large-scale atmospheric circulation. We also examine processes that take place throughout the troposphere (from the low to middle and upper levels), providing thus, more robust results that go beyond the state of the art.

In June to September all models projected increase in Etesians' wind speed ranging from 0.5 to 1 m/s over the same coastal region in late-21c under RCP8.5 (evident in June–August for RCP4.5). Consistent with previous studies, we found that the SLP dipole that controls the Etesians strengthens with increasing forcing in both RCPs (more pronounced in RCP8.5). Climate projections suggest shifts in mean conditions and also changes in climate variability, since the Etesians are forecasting to become more intense (in June to September) and frequent (in May, June, and September).

Under the high-emission scenario and by the end of the twenty-first century, the July to September zonal wind at 200 hPa is generally projected to increase northward of 55°N and southward of 45°N, leading potentially to strengthening of the PJ and STJ. Most of the models project a robust reinforcement of the jet streams, decrease in waviness, and a poleward shift of the STJ.

Overall, our study illustrates that during the Etesians, the European sector exhibits a reinforced westerly flow and a decreased meridional wave amplitude (midlatitude waviness), which might accelerate the eastward progression of the large-scale circulation systems, favoring the establishment of enhanced ridges over the Balkans. In addition, the EMED sector exhibits a stronger 200-hPa zonal flow, and an intensified STJ which shifts poleward by the end of the twenty-first century in both RCPs. Most changes are to a lesser

extent apparent already in mid-21c under both scenarios, with the exception of changes in the meridional circulation index. Finally, all projected changes are more pronounced in September and in late-21c under RCP8.5.

Our results have important societal implications associated with prevention, risk reduction of wildfires, and air pollution. The analysis suggests that the Etesians may significantly increase during summer fire season, and more specifically, the episodes are likely to be more frequent but not longer-lasting than at present. In terms of fire weather threats in the future, this study suggests that the Etesians increases' during critical dry periods, especially late in the extended summer season (September), that could potentially lead to more extensive wildfires in the future. Finally, our results show that climate change will greatly impact the potential for wind energy deployment, which is projected to be significantly increased by the end of the century. Therefore, we suggest policy makers and wind energy companies to take into consideration future climate changes which may alter the pattern and strength of near-surface wind at desirable locations for wind farms over the Aegean.

Acknowledgments
The authors wish to thank Marin Ivanov (GreenPocket, Cologne, Germany), Samuel Somot (Meteo-France/CNRM), Giorgia Di Capua (Potsdam Institute for Climate Impact Research), and George Zittis (The Cyprus Institute) for many suggestions on the former version of this paper and fruitful discussions. In addition, we would like to acknowledge Michel Deque, Clotilde Dubois, and Samuel Somot (CNRM); Grigory Nikulin (SMHI); Fredrik Boberg (DMI); and Robert Vautard and Isabelle Tobin (IPSL) for providing the ALADIN-v5.3, ARPEGE-v5.2, RCA-v4, HIRHAM-v5, and WRF3.3.1 simulations, respectively. Information about how to retrieve the EURO-CORDEX data can be found here: https://euro-cordex.net/. We are indebted to the Hellenic National Meteorological Service for the observational data set that is available here: www.emy.gr. We are grateful to the anonymous reviewers for their valuable comments and suggestions that improved the manuscript. The research leading to these results has received funding from the Deutsche Forschungsgemeinschaft (German Research Foundation) project entitled "The Etesian wind system and energy potential over the Aegean Sea: Past, present, future" with grant LU 1608/7-1.

References

Amraoui, M., Liberato, M., Calado, T., Dacamara, C., Pinto, C. L., Trigo, R., & Gouveia, C. (2013). Fire activity over Mediterranean Europe based on information from Meteosat–8. *Forest Ecology and Management*, *294*, 62–75. https://doi.org/10.1016/j.foreco.2012.08.032

Anagnostopoulou, C., Zanis, P., Katragkou, E., Tegoulias, I., & Tolika, K. (2014). Recent past and future, patterns of the Etesian winds based on regional scale climate model simulations. *Climate Dynamics*, *42*, 1819–1836. https://doi.org/10.1007/s00382-013-1936-0

Barnes, E. A. (2013). Revisiting the evidence linking Arctic amplification to extreme weather in mid-latitudes. *Geophysical Research Letters*, *40*, 4728–4733. https://doi.org/10.1002/grl.50880

Barnes, E. A., & Polvani, L. M. (2015). CMIP5 projections of Arctic amplification, of the North American/North Atlantic circulation, and of their relationship. *Journal of Climate*, *28*, 5254–5271.

Belušić Vozila, A., Güttler, I., Ahrens, B., Obermann-Hellhund, A., & Telišman Prtenjak, M. (2019). Wind over the Adriatic region in CORDEX climate change scenarios. *Journal of Geophysical Research: Atmospheres*, *124*, 110–130. https://doi.org/10.1029/2018JD028552

Bloom, A., Kotroni, V., & Lagouvardos, K. (2008). Climate change impact of wind energy availability in the Eastern Mediterranean using the regional climate model PRECIS. *Natural Hazards and Earth System Sciences*, *8*, 1249–1257.

Cattiaux, J., Peings, Y., Saint–Martin, D., Trou–Kechout, N., & Vavrus, S. J. (2016). Sinuosity of mid-latitude atmospheric flow in a warming world. *Geophysical Research Letters*, *43*, 8259–8268.

Cherchi, A., Annamalai, H., Masina, S., & Navarra, A. (2014). South Asian Summer Monsoon and the Eastern Mediterranean Climate: The Monsoon–Desert Mechanism in CMIP5 Simulations. *Journal of Climate*, *27*, 6877–6903. https://doi.org/10.1175/JCLI-D-13-00530.1

Christensen, O. B., Drews, M., & Christensen, J. H. (2006). The HIRHAM regional climate model version 5. *DMI Technical Report*, *06*, 17–22.

Christidis, N., & Stott, P. A. (2015). Changes in the geopotential height at 500 hPa under the influence of external climatic forcings. *Geophysical Research Letters*, *42*, 10,798–10, 806. https://doi.org/10.1002/2015GL066669

Coumou, D., Di Capua, G., Vavrus, S., Wang, L., & Wang, S. (2018). The influence of Arctic amplification on mid–latitude summer circulation. *Nature Communications*, *9*, 2959. https://doi.org/10.1038/s41467-018-05256-8

Coumou, D., Lehmann, J., & Beckmann, J. (2015). The weakening summer circulation in the Northern Hemisphere mid–latitudes. *Science*, *348*(6232), 324–327. https://doi.org/10.1126/science.1261768

Coumou, D., Petoukhov, V., Rahmstorf, S., Petria, S., & Schellnhuber, H. J. (2014). Quasi–resonant circulation regimes and hemispheric synchronization of extreme weather in boreal summer. *Proceedings of the National Academy of Sciences*, *111*, 12,331–12,336. https://doi.org/10.1073/pnas.1412797111

Dafka, S., Toreti, A., Luterbacher, J., Zanis, P., Tyrlis, E., & Xoplaki, E. (2017). On the ability of RCMs to capture the circulation pattern of Etesians. *Climate Dynamics*, *51*, 1687–1706. https://doi.org/10.1007/s00382-017-3977-2

Dafka, S., Toreti, A., Luterbacher, J., Zanis, P., Tyrlis, E., & Xoplaki, E. (2018). Simulating Extreme Etesians over the Aegean and Implications for Wind Energy Production in Southeastern Europe. *Journal of Applied Meteorology and Climatology*, *57*(5), 1123–1134. https://doi.org/10.1175/JAMC-D-17-0172.1

Dafka, S., Xoplaki, E., Toreti, A., Zanis, P., Tyrlis, E., Zerefos, C., & Luterbacher, J. (2016). The Etesians: from observations to reanalysis. *Climate Dynamics*, *47*, 1569–1585. https://doi.org/10.1007/s00382-015-2920-7

Di Capua, G., & Coumou, D. (2016). Changes in meandering of the Northern Hemisphere circulation. *Environmental Research Letters*, *11*, 1–9.

Ezber, J. (2018). Assessment of the changes in the Etesians in the EURO-CORDEX regional model projections. *International Journal of Climatology*, *39*(3), 1213–1229. https://doi.org/10.1002/joc.5872

Francis, J. A., & Vavrus, S. J. (2012). Evidence linking Arctic amplification to extreme weather in mid-latitudes. *Geophysical Research Letters*, *39*, L06801. https://doi.org/10.1029/2012GL051000

Francis, J. A., & Vavrus, S. J. (2015). Evidence for a wavier jet stream in response to rapid Arctic warming. *Environmental Research Letters*, *10*, 2. https://doi.org/10.1088/1748-9326/10/1/014005

Georgoulias, A. K., Alexandri, G., Kourtidis, K. A., Lelieveld, J., Zanis, P., Pöschl, U., et al. (2016). Spatiotemporal variability and contribution of different aerosol types to the Aerosol Optical Depth over the Eastern Mediterranean. *Atmospheric Chemistry and Physics*, *16*, 13,853–13,884. https://doi.org/10.5194/acp-16-13853-2016

Hartung, K., Svensson, G., & Kjellström, E. (2017). Resolution, physics and atmosphere –ocean interaction – How do they influence climate model representation of Euro-Atlantic atmospheric blocking? *Tellus A: Dynamic Meteorology and Oceanography*, *69*, 1. https://doi.org/10.1080/16000870.2017.1406252

Hochman, A., Harpaz, T., Saaroni, H., & Alpert, P. (2017). Synoptic classification in 21st century CMIP5 predictions over the eastern Mediterranean with focus on cyclones. *International Journal of Climatology*, *38*, 1476–1483. https://doi.org/10.1002/joc.5260

Hueging, H., Haas, R., Born, L., Jacob, D., & Pinto, J. G. (2013). Regional changes in wind energy potential over Europe using regional climate model ensemble projections. *Journal of Applied Meteorology and Climatology*, *52*, 903–917. https://doi.org/10.1175/JAMC-D-12-086.1

Jacob, D., Petersen, J., Eggert, B., Alias, A., Christensen, O. B., Bouwer, L. M., et al. (2014). EURO–CORDEX: New high–resolution climate change projections for European impact research. *Regional Environmental Change*, *14*(2), 563–578. https://doi.org/10.1007/s10113-013-0499-2

Knutti, R., Furrer, R., Tebaldi, C., Cermak, J., & Meehl, G. (2010). Challenges in Combining Projections from Multiple Climate Models. *Journal of Climate*, *23*, 2739–2758. https://doi.org/10.1175/2009JCLI3361.1

Knutti, R., Rugenstein, M., & Hegerl, G. C. (2017). Beyond equilibrium climate sensitivity. *Nature Geoscience*, *10*, 727–736. https://doi.org/10.1038/ngeo3017

Koletsis, I., Kotroni, V., Lagouvardos, K., & Soukissian, T. (2016). Assessment of offshore wind speed and power potential over the Mediterranean and the Black Seas under future climate changes. *Renewable and Sustainable Energy Reviews*, *60*, 234–245.

Koletsis, I., Lagouvardos, K., Kotroni, V., & Bartzokas, A. (2009). The interaction of northern wind flow with the complex topography of Crete Island–Part 1. *Observational study, Natural Hazards and Earth System Sciences*, *9*, 1845–1855.

Kotroni, V., Lagouvardos, K., & Lalas, D. (2001). The effect of the island of Crete on the Etesian winds over the Aegean Sea. *Quarterly Journal of the Royal Meteorological Society*, *127*, 1917–1937.

Logothetis, I., Tourpali, K., Stergios, M., & Zanis, P. (2019). Etesians and the summer circulation over East Mediterranean in Coupled Model Intercomparison Project Phase 5 simulations: Connections to the Indian summer monsoon. *International Journal of Climatology*, 1–14. https://doi.org/10.1002/joc.6259

Mann, M. E., Rahmstorf, S., Kornhuber, K., Steinman, B. A., Miller, S. K., & Coumou, D. (2017). Influence of anthropogenic climate change on planetary wave resonance and extreme weather events. *Scientific Reports*, *7*, 45242. https://doi.org/10.1038/srep45242

Masato, G., Hoskins, B., & Woollings, T. (2013). Winter and summer Northern hemisphere blocking in CMIP5 models. *Journal of Climate*, *26*, 7044–7059.

Matsueda, M., & Endo, H. (2017). The robustness of future changes in Northern Hemisphere blocking: A large ensemble projection with multiple sea surface temperature patterns. *Geophysical Research Letters*, *44*, 5158–5166. https://doi.org/10.1002/2017GL073336

Menut, L., Tripathi, O., Colette, A., Vautard, R., Flaounas, E., & Bessagnet, B. (2013). Evaluation of regional climate simulations for air quality modelling purposes. *Climate Dynamics*, *40*, 2515–2533. https://doi.org/10.1007/s00382-012-1345-9

Moemken, J., Reyers, M., Feldmann, H., & Pinto, J. (2018). Future changes of wind speed and wind energy potentials in EURO–CORDEX ensemble simulations. *Journal of Geophysical Research: Atmospheres*, *123*, 6373–6389. https://doi.org/10.1029/2018JD028473

Moss, R., Edmonds, J. A., Hibbard, K. A., Manning, M. R., Rose, S. K., Van Vuuren, D. P., et al. (2010). The Next Generation of Scenarios for Climate Change Research and Assessment. *Nature*, *463*(7282), 747–756. https://doi.org/10.1038/nature08823

Obermann-Hellhund, A., Conte, D., Somot, S., Torma, C. Z., & Ahrens, B. (2017). Mistral and Tramontane wind systems in climate simulations from 1950 to 2100. *Climate Dynamics*, *50*(1-2), 693–703. https://doi.org/10.1007/s00382-017-3635-8

Peings, Y., Cattiaux, J., Vavrus, S. J., & Magnusdottir, G. (2017). Late twenty–first–century changes in the mid-latitude atmospheric circulation in the CESM large ensemble. *Journal of Climate*, *30*, 5943–5960.

Pfeifer, S., Bülow, K., Gobiet, A., Hänsler, A., Mudelsee, M., Otto, J., et al. (2015). Robustness of Ensemble Climate Projections Analyzed with Climate Signal Maps: Seasonal and Extreme Precipitation for Germany. *Atmosphere*, *6*, 677–698. https://doi.org/10.3390/atmos6050677

Samuelsson, P., Jones, C. G., Will´ En, U., Ullerstig, A., Gollvik, S., Hansson, U. L., et al. (2011). The Rossby Centre Regional Climate model RCA3: model description and performance. *Tellus A*, *63*, 4–23. https://doi.org/10.1111/j.1600-0870.2010.00478.x

Sandeep, S., & Ajayamohan, R. S. (2015). Poleward shift in Indian summer monsoon low level jetstream under global warming. *Climate Dynamics*, *45*, 337–351. https://doi.org/10.1007/s00382-014-2261-y

Skamarock, W. C., Klemp, J. B., Dudhia, J., Gill, D. O., Barker, D. M., Duda, M. G., et al. (2008). A Description of the Advanced Research WRF Version 3. *NCAR Technical Note*, NCAR/TN-475+STR, 113, https://doi.org/10.5065/D68S4MVH

Taylor, K. E., Stouffer, R. J., & Meehl, G. A. (2012). An overview of CMIP5 and the experiment design. *Bulletin of the American Meteorological Society*, *93*, 485–498. https://doi.org/10.1175/BAMS-D-11-00094.1

Tobin, I., Berrisford, P., Dunn, R. J. H., Vautard, R., & McVicar, T. R. (2014). State of climate in 2013. *Bulletin of the American Meteorological Society*, *95*, S28–S29.

Tobin, I., Jerez, S., Vautard, R., Thais, F., van Meijgaard, E., Prein, A., et al. (2016). Climate change impacts on the power generation potential of a European mid–century wind farms scenario. *Environmental Research Letters*, *11*, 034–013. https://doi.org/10.1088/1748-9326/11/3/034013

Tolika, K., Anagnostopoulou, C., Velikou, K., & Vagenas, C. (2015). A comparison of the updated very high resolution model RegCM3_10km with the previous version RegCM3_25km over the complex terrain of Greece: present and future projections. *Theoretical and Applied Climatology*, *126*(3-4), 715–726. https://doi.org/10.1007/s00704-015-1583-y

Tyrlis, E., & Lelieveld, J. (2013). Climatology and dynamics of the summer Etesian winds over the eastern Mediterranean. *Journal of the Atmospheric Sciences*, *70*, 3374–3396. https://doi.org/10.1175/JAS-D-13-035.1

Tyrlis, E., Lelieveld, J., & Steil, B. (2013). The summer circulation over the eastern Mediterranean and the Middle East: influence of the South Asian monsoon. *Climate Dynamics*, *40*, 1103–1123. https://doi.org/10.1007/s00382-012-1528-4

Tyrlis, E., Tymvios, F. S., Giannakopoulos, C., & Lelieveld, J. (2015). The role of blocking in the summer 2014 collapse of Etesians over the eastern Mediterranean. *Journal of Geophysical Research: Atmospheres*, *120*, 6777–6792. https://doi.org/10.1002/2015JD023543

Woollings, T., Barriopedro, D., Methven, J., Son, S. W., Martius, O., Harvey, B., et al. (2018). Blocking and its response to climate change. *Current Climate Change Reports*, *4*(3), 287–300. https://doi.org/10.1029/2018GL079894

Woollings, T., & Blackburn, M. (2012). The North Atlantic Jet Stream under Climate Change and Its Relation to the NAO and EA Patterns. *Journal of Climate*, *25*, 886–902. https://doi.org/10.1175/JCLI-D-11-00087.1

Woollings, T., Hannachi, A., & Hoskins, B. (2010). Variability of the North Atlantic eddy–driven jet stream. *Quarterly Journal of the Royal Meteorological Society*, *649*, 856–868. https://doi.org/10.1002/qj.625

Yim, B. Y., Min, H. S., & Kug, J. S. (2016). Inter-model diversity in jet stream changes and its relation to Arctic climate in CMIP5. *Climate Dynamics*, *47*(1-2), 235–248. https://doi.org/10.1007/s00382-015-2833-5

Zanis, P., Hadjinicolaou, P., Pozzer, A., Tyrlis, E., Dafka, S., Mihalopoulos, N., & Lelieveld, J. (2014). Summertime free–tropospheric ozone pool over the eastern Mediterranean/Middle East. *Atmospheric Chemistry and Physics*, *14*, 115–132. https://doi.org/10.5194/acp-14-1152014,2014